Wartell, R. M., Larson, J. E., & Wells, R. D. (1974) *J. Biol. Chem. 249*, 6719-6732.
Wilson, W. D., Wang, Y.-H., Krishnamoorthy, C. R., & Smith, J. C. (1985) *Biochemistry 24*, 3991-3999.
Wiseman, T., Williston, S., Brandts, J. F., & Lin, L. N. (1989) *Anal. Biochem. 179*, 131-137.
Wolf, B., & Hanlon, S. (1975) *Biochemistry 14*, 1661-1670.
Wu, H.-H., & Crothers, D. M. (1984) *Nature 308*, 509-513.
Zimmer, C. (1975) *Prog. Nucleic Acid Res. Mol. Biol. 15*, 285-318.
Zimmer, C., & Wahnert, U. (1986) *Prog. Biophys. Mol. Biol. 47*, 31-112.

Two-Dimensional NMR Studies on the Anthramycin–d(ATGCAT)$_2$ Adduct†

Thomas R. Krugh,* David E. Graves,‡ and Michael P. Stone§

Department of Chemistry, University of Rochester, Rochester, New York 14627, Department of Chemistry, University of Mississippi, University, Mississippi 38677, and Department of Chemistry, Vanderbilt University, Nashville, Tennessee 37235

Received June 12, 1989

ABSTRACT: Two-dimensional NMR experiments were performed on the adduct of anthramycin with d-(ATGCAT)$_2$ to obtain the assignments of the nucleotide base and sugar protons as well as the anthramycin protons. Anthramycin is covalently attached to a guanine 2-amino group, forming the d(AT^{am}GCAT)·d-(ATGCAT) modified duplex. The anthramycin protons in the minor groove exhibit NOEs to several nucleotide protons. The network of anthramycin-nucleotide NOEs and the measurement of the 10-Hz coupling constant between the anthramycin H11 and H11a protons shows that anthramycin is covalently attached as the *S* stereoisomer at the anthramycin C11 position with the side chain of anthramycin oriented toward the 5′ end of the modified strand. The NOE data show that the anthramycin-modified duplex is in a right-handed conformation with all bases in an anti conformation. Analysis of the $J_{1'-2'}$ coupling constants for the resolved H1′ resonances shows that the S-type conformation of the sugars is highly preferred.

Anthramycin (Figure 1) is a potent antitumor antibiotic which reacts covalently with guanosine-containing duplex DNA to form an adduct that spans a four base pair region [for a review of pyrrolo[1,4]benzodiazepine antibiotics, see Hurley and Needham-VanDevanter (1986)]. Hurley and Petrusek (1979) and Petrusek et al. (1981) concluded that anthramycin forms a minor groove adduct with the exocyclic amino group of guanine. Carbon-13 and proton NMR experiments confirmed this conclusion and demonstrated the anthramycin C11 position as the reactive site (Graves et al., 1984). Subsequent ^{1}H NMR studies were performed on an anthramycin-modified deoxyhexanucleotide, d(AT^{am}G-CAT)·d(ATGCAT), in which anthramycin is covalently attached to the exocyclic amino group of one of the two guanines in the duplex. The other guanine is sterically blocked from reaction with anthramycin, and thus only a 1:1 anthramycin–duplex adduct is formed. These experiments showed that adduct formation had not significantly perturbed the B-DNA conformation and provided insight into solution geometry and dynamics (Graves et al., 1985).

The C11 position of anthramycin could be attacked by the exocyclic amino group of guanine from either face of the molecule, leading to potential formation of *R* and *S* isomers of the adduct. Furthermore, each of these isomers has two potential orientations of the anthramycin side chain in the minor groove (Figure 1). Our previous NMR studies showed that one form of the complex predominates in solution, although the NOESY data were not definitive as to which stereoisomer was formed. Rather, we assumed the formation of the 11(*S*) stereoisomer, as predicted from the model building studies (Petrusek et al., 1981). Subsequent molecular mechanics calculations (Rao et al., 1986; Remers et al., 1986; Zakrewska & Pullman, 1986) found that the lowest energy conformer is one in which anthramycin is bound in the minor groove as the 11(*S*) stereoisomer with the side chain pointing toward the 5′ end of the modified strand.

In the present report, we extend the two-dimensional NMR experiments on the d(AT^{am}GCAT)·d(ATGCAT) modified duplex using a combination of TOCSY and NOESY experiments at 500 MHz [e.g., for reviews see van de Ven and Hilbers (1988) and Nerdal et al. (1988)]. We present coupling constant and NOE data which demonstrate formation of the 11(*S*) adduct and provide assignments for each of the base and most of the sugar protons. In addition, anthramycin-DNA contacts are observed which show that the anthramycin side chain is oriented toward the 5′ end of the modified strand.

Experimental Procedures

Sample Preparation. Anthramycin methyl ether was generously supplied by Professor L. H. Hurley. The deoxyribonucleotide d(ATGCAT)$_2$ was purchased from Pharmacia/P-L Biochemicals. The sample was prepared as described previously (Graves et al., 1985). Briefly, an excess of anthramycin methyl ether was added as a solid to a solution of d-(ATGCAT)$_2$ dissolved in 10 mM sodium phosphate, pH 7.0, 0.1 mM disodium EDTA, and 100 mM sodium chloride. The solution was vigorously mixed for 4 days at 5 °C in the absence of light. The solid anthramycin was then removed from the sample by centrifugation, and unreacted anthramycin was removed via repeated extraction with equal volumes of buffer-saturated 1-butanol. After five extractions, no free an-

† This research was supported in part by U.S. Public Health Service Research Grants CA-35251 (T.R.K.), CA-41474 (D.E.G.), and ES-03755 (M.P.S.).
* Address correspondence to this author at the University of Rochester.
‡ University of Mississippi.
§ Vanderbilt University.

0006-2960/89/0428-9988$01.50/0

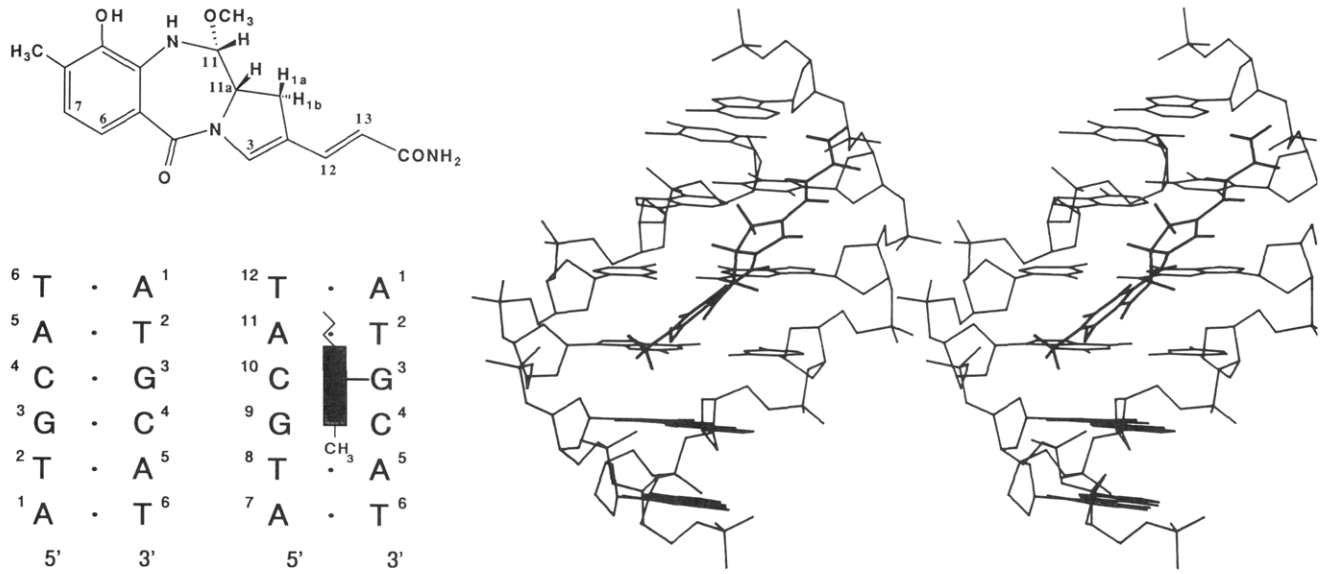

FIGURE 1: (Left panels) The chemical structure of anthramycin (top) and the anthramycin adduct with d(ATGCAT)$_2$ (bottom). The anthramycin is covalently attached to the 2-amino group of one of the guanines, labeled G3; the modified strand is numbered as nucleotides 1–6. (Right panel) Stereo drawing of the anthramycin–d(ATGCAT)$_2$ adduct. Anthramycin is covalently attached to the exocyclic amino group of G3 by an aminal linkage to C11 of anthramycin. This model is based on the B-form of DNA and was kindly provided by Dr. L. H. Hurley.

thramycin was detected in the solution. Sample concentration was 4 mM (strand).

Nuclear Magnetic Resonance. All experiments were performed at 499.84 MHz with a Varian VXR-500S spectrometer. The samples were exchanged three times with D_2O via lyophilization. Samples were maintained at 5 °C and purged with dry nitrogen for 1 min prior to capping. Chemical shifts were referenced to the residual HDO resonance, using a value of 4.85 ppm at 20 °C. The data were processed with Varian software and with the NMR2 software supplied by New Methods Research, Inc. (Syracuse, NY). The spin–spin coupling of the anthramycin resonances was determined by using a phase-sensitive TOCSY pulse sequence (Braunschweiler & Ernst, 1983; Bax & Davis, 1985; Brey, 1988; Glaser et al., 1989), [(delay)–90°–t_1–(spin lock for mixing time)–(acquisition)]$_m$, with mixing times of 70 and 130 ms at 20 and 23 °C. Other parameters used were as follows: a relaxation delay of 3.0 s; 32 transients per t_1 value; 512 complex transients; 2K complex points in t_2; and shifted sine-bell apodization functions. The data were zero-filled in t_1 to give 2K × 2K complex data points. Suppression of the residual water resonance was achieved by saturation during the relaxation delay. Phase-sensitive NOESY spectra were recorded at 20 °C by use of the following parameters: mixing time = 0.450 s; 2K complex data points in t_2; 512 complex data points in t_1; 32 acquisitions per FID; a relaxation delay of 5.0 s; a sweep width of 5000 Hz in both dimensions; a shifted Gaussian apodization function for t_2; and a shifted sine-bell apodization function for the t_1 dimension. Data were also collected with a mixing time of 0.100 s. The data were zero-filled in t_1 to give 2K × 2K complex data points. The residual water resonance was saturated during the relaxation delay.

Results

The downfield portion of the one-dimensional proton NMR spectrum of the anthramycin-modified d(ATGCAT)$_2$ duplex is shown in Figure 2. All of the base protons and more than half of the sugar H1′ protons exhibit well-resolved peaks, as do the anthramycin protons. Formation of d(AT^{am}G-CAT)·d(ATGCAT) removes the 2-fold symmetry of the unmodified d(ATGCAT)$_2$ duplex, which is reflected in the appearance of individual resonances for each of the nucleotide

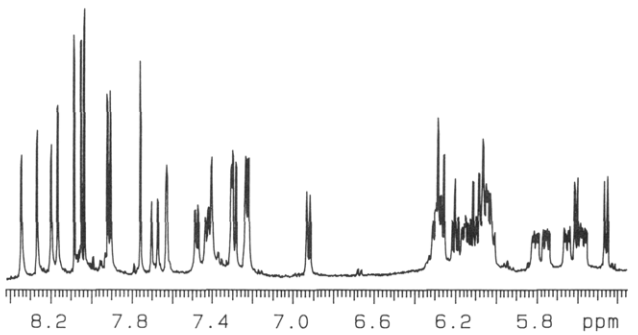

FIGURE 2: Downfield portion of the ^{1}H spectra at 500 MHz of the anthramycin–d(ATGCAT)$_2$ modified duplex at 20 °C.

Table I: Chemical Shifts of Anthramycin Protons in the Anthramycin–d(ATGCAT)$_2$ Modified Duplex[a]

anthramycin proton	chemical shift	anthramycin proton	chemical shift
CH_3	2.45	H7	6.93
H1a	3.86	H11	6.08
H1b	3.57	H11a	4.48
H3	7.63	H12	7.69
H6	7.29	H13	6.29

[a] Values given are in ppm referenced to internal TSP.

protons. The resolution obtained at 500 MHz permits the assignment of the nucleotide and anthramycin protons and provides unequivocal evidence on the stereochemistry and orientation of the anthramycin moiety in the d(AT^{am}G-CAT)·d(ATGCAT) duplex.

Assignment of the Anthramycin Protons. The anthramycin H3, H6, H7, H12, H13, and CH_3 protons in the modified duplex were assigned previously (Graves et al., 1984, 1985); these assignments are verified by the present results. The previously unassigned anthramycin H11, H11a, H1a, and H1b protons in the modified duplex are assigned by TOCSY experiments (see Figure 3) and are listed in Table I. The two protons at the C1 position of anthramycin are nonequivalent and are labeled as H1a and H1b; we define H1a to lie on the same face of anthramycin as H11a. The anthramycin H3 resonance exhibits broader lines than the anthramycin H12 resonance in the one-dimensional spectrum (Figure 3, top) due

Table II: Chemical Shifts of the Nucleotide Protons in the Anthramycin–d(ATGCAT)$_2$ Duplex[a]

base	H8	H6	H1′	H2′	H2″	H3′	H4′	H5′,5	H2/H5	CH_3
A1	8.18		6.31	2.70	2.98	4.94	4.15	*b*	8.06	
T2		7.42	5.57	2.36	2.49	4.96	4.22	*b*		1.49
G3	7.92		6.07	2.50	2.81	5.01	4.15	*b*		
C4		7.45	5.81	2.17	2.45	4.90	3.79	3.92, 4.22	5.47	
A5	8.21		6.16	2.51	2.84	4.80	2.90	3.30, 3.68	8.04	
T6		7.25	6.22	2.14	2.17	4.58	4.07	4.12, 4.28		1.47
A7	8.28		6.28	2.68	2.89	4.92	4.3	*b*	8.09	
T8		7.32	5.76	2.17	2.49	4.91	4.25	*b*		1.45
G9	7.93		5.65	2.70	2.48	5.01	4.38	*b*		
C10		7.49	6.06	2.08	2.46	4.98	4.41	*b*	5.62	
A11	8.36		6.04	2.68	2.68	4.84	3.29	3.17, 3.85	7.77	
T12		7.23	6.12	2.13	2.05	4.52	3.63	3.87, 4.07		1.40

[a] Values given are in ppm referenced to TSP. [b] The unassigned H5′,5″ protons overlap in the 4.1–4.3 ppm region.

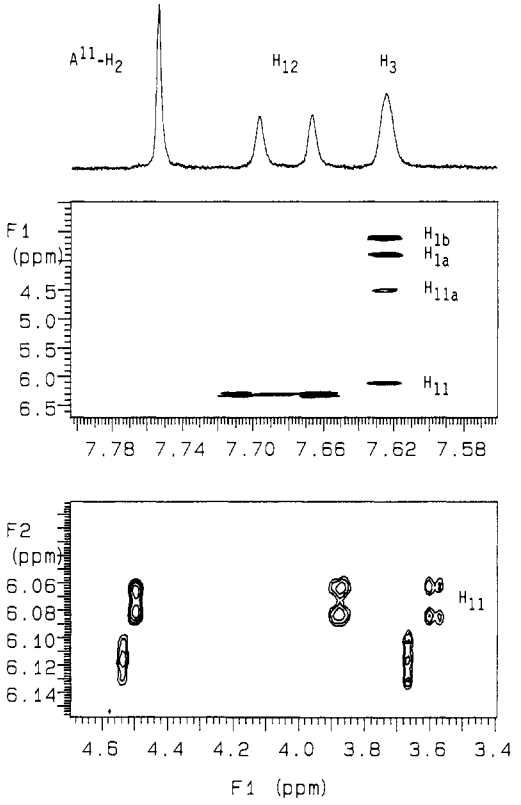

FIGURE 3: (Top) The 7.56–7.80 ppm section of the one-dimensional proton spectrum of the anthramycin–d(ATGCAT)$_2$ duplex. The anthramycin H12 resonance is a doublet due to a 15.3-Hz coupling between the anthramycin H12 and anthramycin H13 protons. (Middle) TOCSY spectrum recorded at 23 °C illustrating the connectivity between the anthramycin H3 and other anthramycin protons. (Bottom) Region of the TOCSY spectrum containing the cross-peaks from anthramycin H11 at 6.08 ppm to anthramycin H11a at 4.48 ppm, anthramycin H1a at 3.86 ppm, and anthramycin H1b at 3.57 ppm. The 10-Hz doublet of the anthramycin H11 resonance is evident in the TOCSY data.

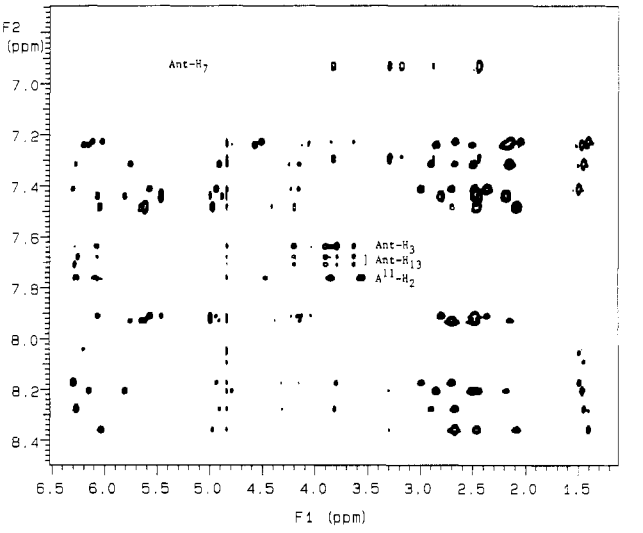

FIGURE 4: A portion of the phase-sensitive NOESY spectrum of anthramycin–d(ATGCAT)$_2$ recorded at 20 °C with a mixing time of 0.45 s. The cross-peaks from the anthramycin H7, anthramycin H3, anthramycin H13, and adenine-11 H2 protons are indicated.

to unresolved spin–spin coupling. However, these unresolved couplings are sufficient for the observation of strong TOCSY cross-peaks to anthramycin H11, H11a, H1a, and H1b, illustrating the utility of TOCSY experiments.

Figure 3 (bottom) shows cross-peaks between anthramycin H11, located at 6.08 ppm, and anthramycin H11a at 4.48 ppm. These data show that the vicinal coupling between these protons is 10 Hz, indicative of the trans configuration. In addition, cross-peaks are observed between H11 and both anthramycin H1a and H1b at 3.86 and 3.57 ppm, respectively (Figure 3). The resonance at 3.86 ppm is assigned as H1a on the basis of the observation of a stronger NOE to H11a when compared to the NOE observed with the proton resonance at 3.57 ppm. Anthramycin H1b exhibits a doublet splitting pattern due to spin–spin coupling to H1a. This suggests that the coupling constant between the H1b and H11a protons is small (<4 Hz), presumably reflecting the dihedral angle dependence of the coupling constant of vicinal protons. The anthramycin H1a cross-peak is an unresolved multiplet in the NOESY and TOCSY spectra due to coupling to both anthramycin H11a and H1b.

Assignments for the Base and Sugar Protons. The loss of symmetry upon adduct formation allows a complete set of connectivities from both the modified and unmodified strands to be resolved in NOESY experiments (Figure 4). The base-to-H1′ portion of the NOESY spectrum is shown in Figure 5, along with the connectivities used to make the assignments, which are collected in Table II. The two adenine H8 resonances from the 5′-terminal nucleotides are readily identified through observation of NOEs to their own sugar H1′ protons but not to a 5′-neighbor H1′ proton. Knowledge of the sequential sugar H1′ assignments allows the corresponding H2′, H2″, H3′, and H4′ protons in each nucleotide unit to be assigned from inspection of TOCSY data and NOESY data at 100-ms mixing time. The H5′,5″ protons remain incompletely assigned due to spectral overlap.

Assignment of the Modified and Unmodified Strands. Although each strand may be individually traced from its 5′ to 3′ end, determination of which strand contains the covalently bound anthramycin requires additional analysis. Utilization of the palindromic sequence d(ATGCAT) precludes the use

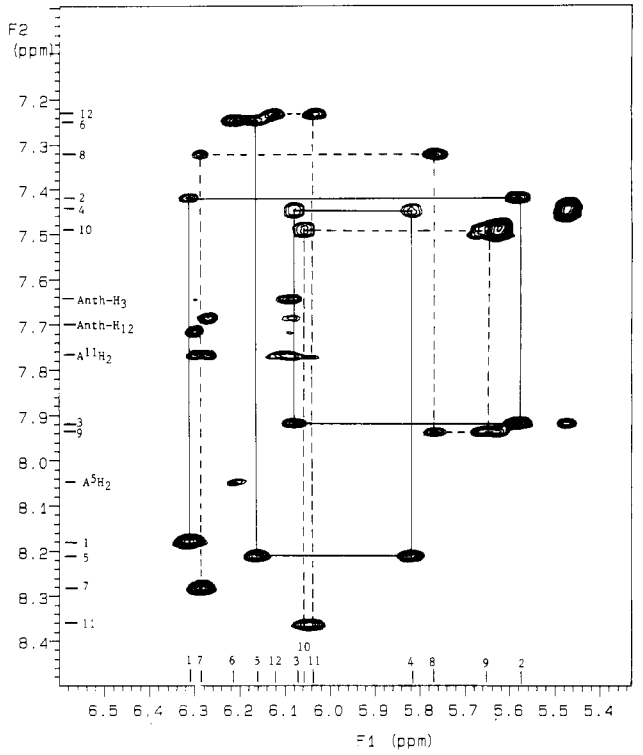

FIGURE 5: The base-to-H1′ region of the NOESY spectrum showing the connectivities used for the assignments of the base and sugar H1′ protons. The locations of the base and sugar H1′ protons are shown along the left edge and bottom edge of the figure, respectively. The solid lines trace out the connectivities of the modified strand, and the dashed lines trace out the connectivities of the unmodified strand.

of the nucleotide–nucleotide NOE connectivities to differentiate between the two strands of the modified duplex. Assignment of the modified guanine (i.e., which of the guanines is G3) requires identification of NOEs between anthramycin protons and DNA protons that are unique to either the modified or unmodified strand. The observation of specific NOEs between the anthramycin and nucleotide protons, which will be discussed in the following paragraph, provides unequivocal assignment of the modified and unmodified strands. In this analysis, we assume only that formation of d(AT^{am}GCAT)·d(ATGCAT) does not result in severe distortion of the B-DNA conformation. This assumption is reasonable and is based upon the present and previous NMR studies (Graves et al., 1984, 1985) which demonstrated (1) an increase in T_m upon adduct formation, (2) the presence of 6 hydrogen-bonded base pairs, (3) NOE contacts between thymine methyl protons and adenine H8 protons, and (4) a complete set of base-to-H1′ NOE connectivities for each strand of the modified duplex.

A strong NOE is observed between a cytosine H1′ and anthramycin H11, as shown in Figure 6. NOESY and TOCSY data demonstrated the configuration at C11 to be *S*, with H11 and H11a trans and pointing toward opposite DNA strands. Observation of this strong NOE is consistent only with C4-H1′ because no reasonable orientation of anthramycin would allow close contact between anthramycin H11 and C10-H1′. Thus, we assign this H1′ to be C4-H1′. This assignment of C4-H1′ is substantiated by observation of a strong NOE between anthramycin H11a (4.48 ppm) and an internal adenine H1′ (6.04 ppm), as shown in Figure 6. The base to sugar H1′ NOEs (Figure 5) clearly identify this adenine H1′ as an internal adenine which is on the complementary strand to the C4-H1′ resonance assigned above. Thus this adenine H1′ resonance can only be A11-H1′. A strong NOE is observed from anthramycin H13 to a terminal thymidine H1′ (Figure 6). The base-to-H1′ NOE data reveal that this thymidine H1′ is on the same strand as the A11-H1′ and thus is assigned as the T12-H1′ resonance.

Conformation of the Deoxyribose Sugars. The one-dimensional proton spectrum of the d(AT^{am}GCAT)·d(ATGCAT) modified duplex (Figure 2) exhibits several well-resolved sugar H1′ resonances from which we may extract the values of $J_{1'-2'}$ and $J_{1'-2''}$ as well as the sum of $J_{1'-2'}$ and $J_{1'-2''}$ ($\sum$1′ in Table III) to determine the conformation of the deoxyribose ring [e.g., Rinkel and Altona (1987), Saenger (1984), Zhou et al. (1988), and Wolk et al. (1989)]. The sum of $J_{1'-2'}$ and $J_{1'-2''}$ for the H1′ resonances is measured as the spacing between the two outermost peaks, while the individual values of $J_{1'-2'}$ and $J_{1'-2''}$ are measured from the spacings between peaks. The terminal thymidine H1′ resonances (T6 and T12) exhibit a triplet structure, and thus the coupling constants were estimated from a comparison of experimental and simulated spectra. The values of $\sum$1′ are greater than 14.5 Hz for the T2, G3, C4, A5, T8, G9, and A11 sugars which, according to Rinkel and Altona (1987), shows that the S-type conformation is strongly preferred; the $J_{1'-2'}$ coupling constants for A1, T2, G3, C4, A5, T8, and G9 are >9 Hz, also indicative of the formation of the S-type conformation. Values of $J_{1'-2'}$ greater than 10 Hz and $J_{1'-2''}$ less than 4.5 Hz for the T2, C4,

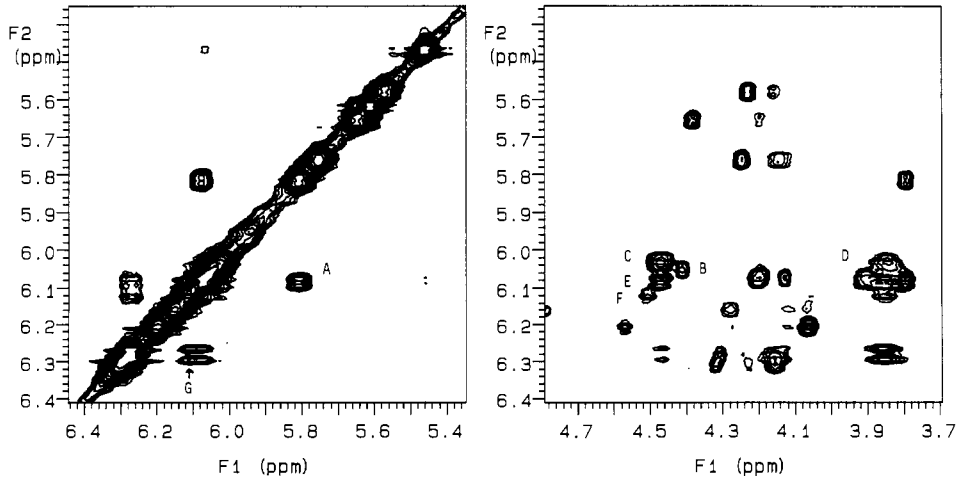

FIGURE 6: Two sections of the phase-sensitive NOESY spectrum of the anthramycin–d(ATGCAT)$_2$ modified duplex. Anthramycin to nucleotide NOEs are labeled as follows: (A) anthramycin H11 to C4-H1′; (B) C10-H1′ to C10-H4′; (C) A11-H1′ to anthramycin H11a; (D) A11-H1′ to anthramycin H1a; (E) anthramycin–H11 to anthramycin H11a; (F) T12-H1′ to T12-H3′; (G) anthramycin H13 to T12-H1′.

Table III: $J_{1'-2'}$ and $J_{1'-2''}$ Coupling Constants[a]

sugar	$\sum 1'$[b]	$J_{1'-2'}$	$J_{1'-2''}$
A1	c	8.9	6.3
T2	14.8	10.8	4.0
G3	15.2[d]	9.8[d]	5.5[d]
C4	15.2	10.8	4.2
A5	15.0	9.1	6.0
T6	14.7	7.8[e]	6.8[e]
T8	15.2	10.0	5.2
G9	14.8	10.8	4.0
A11	15.4[f]	f	f
T12	14.5	7.8[e]	6.7[e]

[a] Measured from a one-dimensional spectrum at 23 °C. The values are given in Hz with estimated uncertainties of ±0.4 Hz. [b] The value listed as $\sum 1'$ is the sum of $J_{1'-2'} + J_{1'-2''}$ and is the separation of the two outermost peaks of the multiplet. [c] Overlap of one component of multiplet. [d] The G3-H1′ resonance occurs in the crowded 6.0–6.1 ppm region, and thus the coupling constants for the G3-H1′ proton are from a measurement of the difference spectrum obtained upon irradiation of the G3-H2″ proton (estimated error ±0.6 Hz). [e] The T6-H1′ and T12-H1′ protons are pseudotriplets, and thus the values of $J_{1'-2'}$ and $J_{1'-2''}$ were determined from comparison of experimental and simulated spectra (estimated uncertainty ±0.6 Hz). [f] The A11-H1′ resonance occurs in the crowded 6.0–6.1 ppm region; irradiation of the overlapped A11-H2′,H2″ resonances at 2.68 ppm gave an NOE difference spectrum showing the A11-H1′ resonance at 6.04 ppm which was used for the measurement of $\sum 1'$. The A11-H1′ resonance has the appearance of a "pseudotriplet".

and G9 sugars are unusual for DNA oligomers and may reflect an unusually large sugar pucker. However, spectral overlap and line broadening accompanying adduct formation precluded measurement of the splitting of the 2′ and 2″ resonances, and thus a complete interpretation of the deoxyribose sugar conformation is deferred. The $J_{1'-2'}$ coupling constants from the 3′-terminal thymidine H1′ resonances are in the 7–8-Hz range, reflecting either a slightly different pseudorotation angle, an equilibrium mixture of sugar conformations, or both. On the other hand, the coupling constants and fine structure of the H1′ resonances show clearly that the T2, G3, C4, A5, T8, and G9 sugars in the anthramycin-modified duplex exhibit an S-type conformation, with no indication of the mixture of N and S conformations frequently found in DNA oligomers [e.g., Rinkel and Altona (1987), Saenger (1984), Zhou et al. (1988), and Wolk et al. (1989)] and likely present at the terminal bases (e.g., A1, T6, A7, and T12) in d(AT^{am}GCAT)·d(ATGCAT).

Discussion

A distinguishing feature of pyrrolo[1,4]benzodiazapine antitumor agents first noted by Hurley and co-workers (Petrusek et al., 1981) is their ability to form tight minor groove complexes with DNA. Both CPK model building (Petrusek et al., 1981) and more recent molecular mechanics calculations (Rao et al., 1986; Remers et al., 1986; Zakrzewska & Pullman, 1986) conclude that the stereochemistry and orientation of binding occur predominantly (if not exclusively) in only one manner. All previous experimental studies of anthramycin have yielded results consistent with formation of the 11(*S*) isomer at the anthramycin C11 position and the rotational isomer in which the aromatic ring of anthramycin is oriented in the 3′ direction from the modified guanine base. NMR spectroscopy of defined anthramycin–oligodeoxynucleotide adducts can unequivocally define the stereochemistry and orientation of binding. In our initial 2D NMR studies on the d(AT^{am}GCAT)·d(ATGCAT) modified duplex (Graves et al., 1985), the spectral complexity at 400 MHz, combined with instrumental limitations, precluded the assignment of all of the base and sugar protons, which limited the interpretation of the data. For example, we did not obtain sufficient NOE data to define the stereochemistry at C11, and the orientation of the anthramycin within the minor groove was based upon the observation of a single NOE. The present results represent a significant extension of the previous work and provide unequivocal evidence in support of the original model of Hurley and co-workers (Petrusek et al., 1981), a conclusion consistent with our previous interpretation of the more limited NOE data.

Formation of d(AT^{am}GCAT)·d(ATGCAT). The asymmetric carbon at the anthramycin C11a position provides the molecule with a 45° right-handed twist between the aromatic and pyrrolo ring (Mostad et al., 1978). The DNA-reactive moiety is the N10, C11 carbinolamine functionality, which, in the case of anthramycin methyl ether, undergoes facile interconversion between the 11(*R*) and 11(*S*) isomers in aqueous solution (Thurston & Langley, 1986). The intermediate N10, C11 imine is likely to be the reactive species that bonds to DNA. In the transition state leading to adduct formation, attack by the exocyclic amino group of guanine could occur from either face, leading to formation of a mixture of 11(*R*) and 11(*S*) DNA adducts. Furthermore, two rotational isomers of the drug in relationship to the minor groove are possible for each stereoisomer, i.e., with the anthramycin C12–C13 side chain oriented toward either the 3′ or 5′ end of the modified strand.

Upon close inspection, the spectrum exhibits small resonances with amplitudes less than 5% of the main resonances. These small peaks could indicate the presence of the 11(*R*) enantiomer, or rotational isomers of the adduct, or the presence of a small amount of unreacted $d(ATGCAT)_2$, or possibly a small amount of degradation of the adduct. We are unable at present to provide a definitive interpretation as to the origin of these small peaks, but their presence does not affect interpretation of the spectrum arising from the major component of the sample. Clearly, the reaction between anthramycin and guanine NH_2 proceeds predominantly, if not exclusively, via a single transition state and leads to formation of only one adduct. No changes in the spectrum were observed over the course of the investigation, which indicates that the lowest energy conformation was achieved.

Structure of the Anthramycin Adduct with $d(ATGCAT)_2$. Two key factors determine the basic structure of the anthramycin adduct. These are (1) the stereochemistry at anthramycin C11, and (2) the orientation of the anthramycin side chain in the minor groove. In the present study we demonstrate that both factors can be defined directly from the NMR spectrum.

Evidence for the existence of the 11(*S*) stereoisomer at anthramycin C11 is derived from NOESY and TOCSY spectral data. In the TOCSY spectrum of d(AT^{am}GCAT)·d(ATGCAT) the vicinal coupling between anthramycin H11 and H11a protons is 10 Hz, which is consistent with formation of the 11(*S*) stereoisomer. Hurley and co-workers (personal communication) have obtained independent evidence supporting the presence of the 11(*S*) conformation in the d(AT^{am}GCAT)·d(ATGCAT) modified duplex from the observation of a COSY cross-peak between H11 and H11a, indicative of a large coupling constant.

Unambiguous evidence for the formation of the 11(*S*) stereoisomer is obtained in the NOESY spectrum from anthramycin–anthramycin intramolecular NOEs and from anthramycin to DNA NOEs. In the 11(*S*) isomer the anthramycin H11 and anthramycin H11a protons are oriented toward opposite strands of the oligodeoxynucleotide whereas in the 11(*R*) stereoisomer the anthramycin H11 and H11a protons are oriented toward the same strand. As noted above,

the anthramycin H11 proton exhibits a strong NOE to the C4-H1′ proton while anthramycin H11a exhibits a strong NOE to the A11-H1′ proton. These cross-strand NOEs are unequivocal evidence for formation of the 11(*S*) stereoisomer. Furthermore, in the 11(*S*) (trans) stereoisomer, the H11 and H11a protons are on opposite sides of the ring and thus are not expected to exhibit a strong NOE, whereas in the 11(*R*) conformation, both protons would lie on the same side of the anthramycin ring, which should result in a strong NOE. In a 100-ms mixing time NOESY experiment we observe only a weak NOE between the anthramycin H11 and anthramycin H11 protons, consistent with formation of the 11(*S*) isomer.

Molecular mechanics calculations indicate that orientation of the anthramycin C12–C13 side chain toward the 5′ end of the modified strand is favored by 5 kcal/mol (Rao et al., 1986) or 9.3 kcal/mol (Remers et al., 1986) as compared to the opposite orientation in which the side chain points toward the 3′ end of the modified strand. Zakrzewska and Pullman (1986) did not report a value for the energy difference but indicated that the 3′ orientation for anthramycin binding to a dG·dC duplex was extremely disfavored. The strong NOEs observed between anthramycin H1a and H1b protons and the A11-H2 proton show that the orientation of the anthramycin C12–C13 side chain is toward the 5′ end of the modified strand, as predicted by theory. The A5-H2 proton is too far away from the anthramycin H1a and H1b protons to exhibit strong NOEs even if the anthramycin were oriented in the opposite direction. Observation of an NOE between the anthramycin H13 proton and the T12-H1′ proton also supports the conclusion that the side chain points toward the 5′ end of the modified strand. If the side chain pointed toward the 3′ end of the modified strand, the H13 proton would be more than 5 Å from either terminal T-H1′ proton and thus would not exhibit an NOE. Thus, we conclude that the drug moiety is held tightly in one orientation, presumably stabilized by formation of hydrogen-bonding interactions between the drug and the oligodeoxynucleotide (Petrusek et al., 1981).

We previously reported an NOE between the anthramycin methyl and A5-H2 protons (Graves et al., 1985) which was cited as evidence for the orientation of the anthramycin methyl group toward the 3′ end of the modified strand. This NOE also was observed in cross sections of the present experiments, although it is weak, indicative of a long-range dipolar interaction ($r > 4.0$ Å).

Graves et al. (1985) also noted several NOEs from unusually high-field resonances (e.g., see Figure 4 in this paper) which were tentatively assigned in our earlier studies as arising from H4′ and H5′,5″ protons. As noted in Table II and under Results, these resonances have now been assigned. The unusual chemical shifts of several nucleotide protons reflect the presence of anthramycin in the minor groove.

Orientation of the Anthramycin Side Chain. The single bond between anthramycin C2 and C12 allows for possible rotation of the side chain. The C12–C13 nuclei of the side chain are expected to be coplanar with the five-membered ring to allow for conjugation of the anthramycin C2–C3 and anthramycin C12–C13 double bonds. In Figure 1, anthramycin H12 is shown pointing in the direction of the anthramycin H3, while anthramycin H13 points into the minor groove. The alternate planar conformation would have H12 pointing into the minor groove while H13 would point out of the minor groove. Anthramycin H13 shows a strong NOE to A11-H2, indicating a conformation in which anthramycin H13 is located deep in the minor groove, as shown in Figure 1. Anthramycin H12 does not exhibit an NOE to A11-H2, whereas a strong NOE would be expected if anthramycin H12 faced into the minor groove. In addition, anthramycin–anthramycin NOEs provide indepedent evidence for the conformation of the side chain, as strong NOEs are observed between anthramycin H13 and H1a and H1b protons, consistent with the orientation of the side chain as shown in Figure 1. Likewise, the anthramycin H3 proton exhibits an NOE to the anthramycin H12 proton, but not to the anthramycin H13 proton. Also, the anthramycin H12 proton does not exhibit an NOE to the anthramycin H1a and H1b protons, which rules out conformations in which the anthramycin H12 proton might be close to the anthramycin H1a and H1b protons.

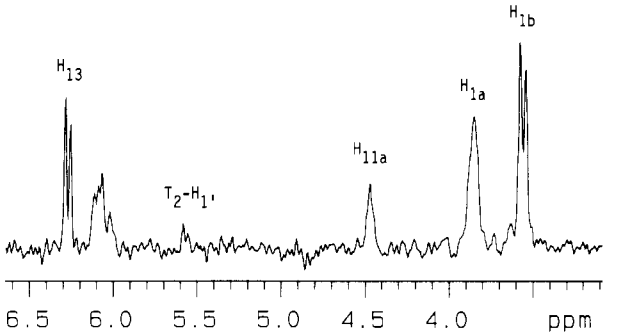

FIGURE 7: Slice from the NOESY spectrum for the A11-H2 proton. Cross-peaks are labeled in the figure, with the exception of the overlapped cross-peaks at 6.04–6.13 ppm which consist of cross-peaks from T12-H1′ (6.12 ppm), anthramycin H11 (6.08 ppm), G3-H1′ (6.07 ppm), and A11-H1′ (6.04 ppm).

Minor Groove Drug–DNA Interactions. The four adenine H2 protons were previously assigned from analysis of melting, nonselective T_1 relaxation, and 1D NOE data (Graves et al., 1984, 1985). Direct confirmation of these assignments is derived from long-range NOEs between specific A-H2 protons and adjacent H1′ protons assigned above. The presence of the bound anthramycin within the minor groove results in close contacts between the A11-H2 proton and the anthramycin H1a, H1b, H11a, and H13 protons (Figure 7). These contacts are consistent with the previous nonselective T_1 relaxation measurements which showed a significant decrease in T_1 for A11-H2, accompanied by increased shielding (0.27 ppm).

Increased shielding is also observed for specific sugar protons. T2-H1′ is ~0.2 ppm upfield of T8-H1′, G9-H1′ is ~0.5 ppm upfield of G3-H1′, and C4-H1′ is ~0.25 ppm upfield from C10-H1′. The presence of anthramycin results in a large increase in shielding for the internal adenine H4′, H5′, H5″ protons (Table II), as previously predicted (Graves et al., 1985). In contrast, less variation in chemical shift is observed between corresponding sets of H2′ and H3′ protons on the two strands. In B-form DNA these protons face the major groove and thus are not expected to be sensitive to adduct formation in the minor groove.

Geometry of the Modified Duplex. The well-defined NOESY cross-peaks for the base-to-sugar protons (Figure 5) make it clear that the conformation of the DNA is not severely altered by attachment of anthramycin at the G3 NH_2 group in d(ATGCAT)$_2$. The relative magnitudes of the base to sugar H1′ cross-peaks and the base to sugar H2′,H2″ cross-peaks in NOESY spectra with a 100-ms mixing time indicate that the duplex is right-handed with all of the bases in an anti conformation (i.e., a B-type duplex). The coupling constants of the sugar H1′ resonances are also consistent with this conclusion. The present data show many other NOE contacts between anthramycin and the nucleotide protons (e.g., see Figure 4 where the cross-peaks between the anthramycin H12, H13, H3, H6, H7, and H11a protons and sugar and adenine

H2 protons are visible). We conclude that the major conformational features of the adduct are reasonably well modeled by the structure in Figure 1. However, anthramycin does interact with the oligomer, and thus we expect to find small, but important, deviations from a standard B-DNA helix. Although the key structural features such as the formation of the 11(*S*) stereoisomer and the orientation of the anthramycin side chain are unequivocal from the present data, additional experiments are in progress to obtain the necessary NOESY buildup curves for subsequent three-dimensional structure analysis of anthramycin-modified duplexes.

Added in Proof

After submission of this paper, we received a manuscript from Dr. Laurence H. Hurley describing two-dimensional NMR experiments on the anthramycin–d(ATGCAT)$_2$ adduct. The conclusions of Hurley and co-workers (Boyd et al., 1990) are in agreement with the results described above.

Acknowledgments

The Varian 500-MHz NMR spectrometer was purchased with support from the National Institutes of Health (RR-03317) and the National Science Foundation (BBS-86-11927).

References

Bax, A., & Davis, D. G. (1985) *J. Magn. Reson. 65*, 355.

Boyd, F. L., Cheatham, S. F., Remers, W., Hill, G. C., & Hurley, L. H. (1990) *J. Am. Chem. Soc.* (in press).

Braunschweiler, L., & Ernst, R. R. (1983) *J. Magn. Reson. 71*, 521.

Bray, W. S. (1988) *Pulse Methods in 1D and 2D Liquid-Phase NMR*, pp 528–531, Academic Press, New York.

Glaser, S. J., Remerowski, M. L., & Drobny, G. P. (1989) *Biochemistry 28*, 1483–1487.

Graves, D. E., Pattaroni, C., Krishnan, B. S., Ostrander, J. M., Hurley, L. H., & Krugh, T. R. (1984) *J. Biol. Chem. 259*, 8202–8209.

Graves, D. E., Stone, M. P., & Krugh, T. R. (1985) *Biochemistry 24*, 7573–7581.

Hertzberg, R. P., Hecht, S. M., Reynolds, V. L., Molineux, I. J., & Hurley, L. H. (1986) *Biochemistry 25*, 1249–1258.

Hurley, L. H., & Petrusek, R. L. (1979) *Nature (London) 282*, 529–531.

Hurley, L. H., & Needhan-VanDevanter, D. R. (1986) *Acc. Chem. Res. 19*, 230–237.

Nerdal, W., Hare, D. R., & Reid, B. R. (1988) *J. Mol. Biol. 201*, 717–739.

Petrusek, R. L., Anderson, G. L., Garner, T. F., Fannin, Q. L., Kaplan, D. J., Zimmer, S. G., & Hurley, L. H. (1981) *Biochemistry 20*, 1111–1119.

Rao, S. N., Singh, U. C., & Kollman, P. A. (1986) *J. Med. Chem. 29*, 2484–2492.

Remers, W. A., Mabilia, M., & Hopfinger, A. J. (1986) *J. Med. Chem. 29*, 2492–2503.

Rinkel, L. J., & Altona, C. (1987) *J. Biomol. Struct. Dyn. 4*, 621–649.

Saenger, W. (1984) *Principles of Nucleic Acid Structure*, Springer-Verlag, New York.

Thurston, D. E., & Langley, D. R. (1986) *J. Org. Chem. 51*, 705–712.

Ughetto, G., Wang, A. H.-J., Quigley, G. J., van der Marel, G. A., van Boom, J. H., & Rich, A. (1985) *Nucleic Acids Res. 13*, 2305–2323.

van de Ven, F. J. M., & Hilbers, C. (1988) *Eur. J. Biochem. 178*, 1–38.

Wang, A. H.-J., Ughetto, G., Quigley, G. J., Hakoshima, T., van der Marel, G. A., van Boom, J. H., & Rich, A. (1984) *Science 225*, 1115–1121.

Wolk, S. W., Thurmes, W. N., Ross, W. S., Hardin, C. C., & Tinoco, I., Jr. (1989) *Biochemistry 28*, 2452–2459.

Zakrzewska, K., & Pullman, B. (1986) *J. Biomol. Struct. Dyn. 4*, 127–136.

Zhou, N., Manogaran, S., Zon, G., & James, T. L. (1988) *Biochemistry 27*, 6013–6020.